Supporting Information

Difference and Influence of Inactive and Active States of Cannabinoid Receptor Subtype CB2: From Conformation to Drug Discovery

Jianping Hu ‡[1, 2, 3], Zhiwei Feng ‡[1], Shifan Ma[1], Yu Zhang[1], Qin Tong[1], Mohammed Hamed Alqarni[1], Xiaojun Gou[3], and Xiang-Qun Xie[1, *]

[1]Department of Pharmaceutical Sciences and Computational Chemical Genomics Screening Center, School of Pharmacy; NIH National Center of Excellence for Computational Drug Abuse Research; Drug Discovery Institute; Department of Computational Biology and Structural Biology, School of Medicine, University of Pittsburgh, Pittsburgh, Pennsylvania 15260, United States. E-mail: xix15@pitt.edu

[2] College of Chemistry, Leshan Normal University, Leshan, Sichuan 614004,China

[3]School of Pharmacy and Bioengineering; Key Laboratory of Medicinal and Edible Plants Resources Development, Chengdu University, Chengdu, Sichuan 610106, China

‡ These authors equally contributed to this work.

***Corresponding Author: Xiang-Qun (Sean) Xie, MBA, Ph.D.**

Professor of Pharmaceutical Sciences/Drug Discovery Institute

Director of CCGS and NIDA CDAR Centers

335 Sutherland Drive, 206 Salk Pavilion

University of Pittsburgh

Pittsburgh, PA15261, USA

412-383-5276 (Phone)

412-383-7436 (Fax)

Email: xix15@pitt.edu

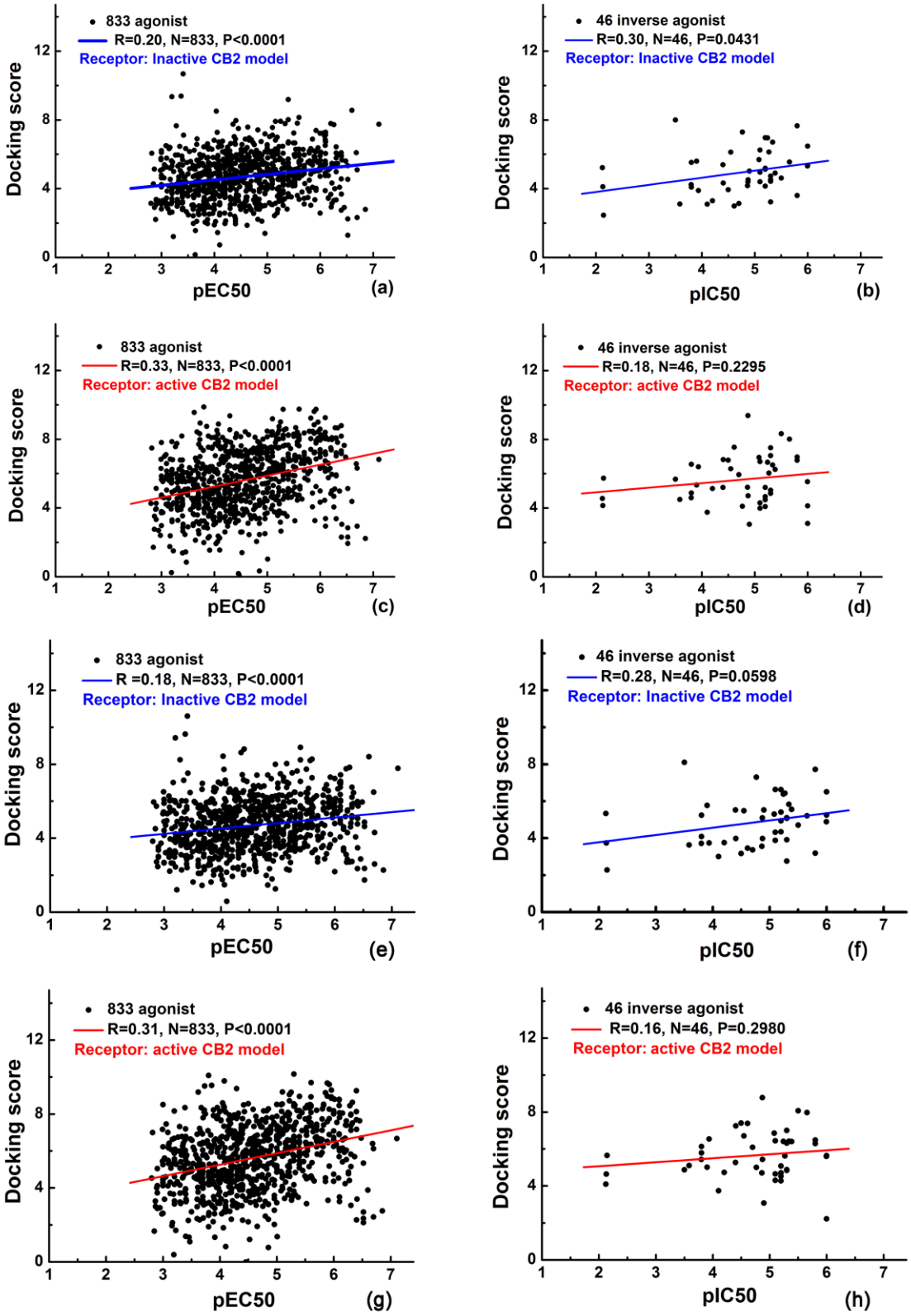

Figure S1. Prescreen validation of other two active and inactive CB2 models. (a-b) Inactive CB2 model 2, (c-d), active CB2 model 2, (e-f) inactive CB2 model 3, (g-h) active CB2 model 3.

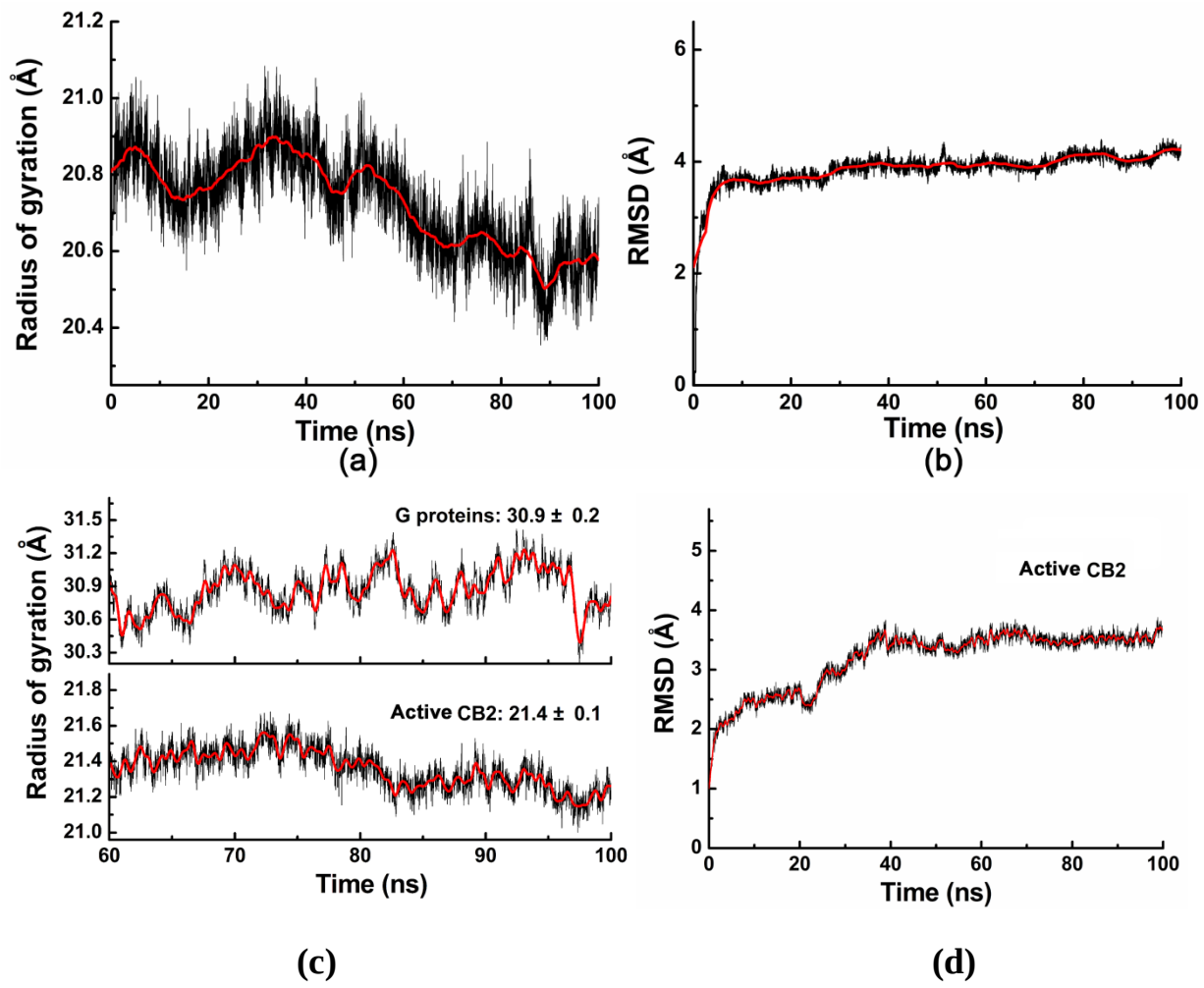

Figure S2. The overall MD parameters of the inactive or active CB2 system. (a) Radius of gyration of inactive CB2, (b) RMSD of inactive CB2, (d) Radius of gyration of active CB2, (d) RMSD of active CB2.

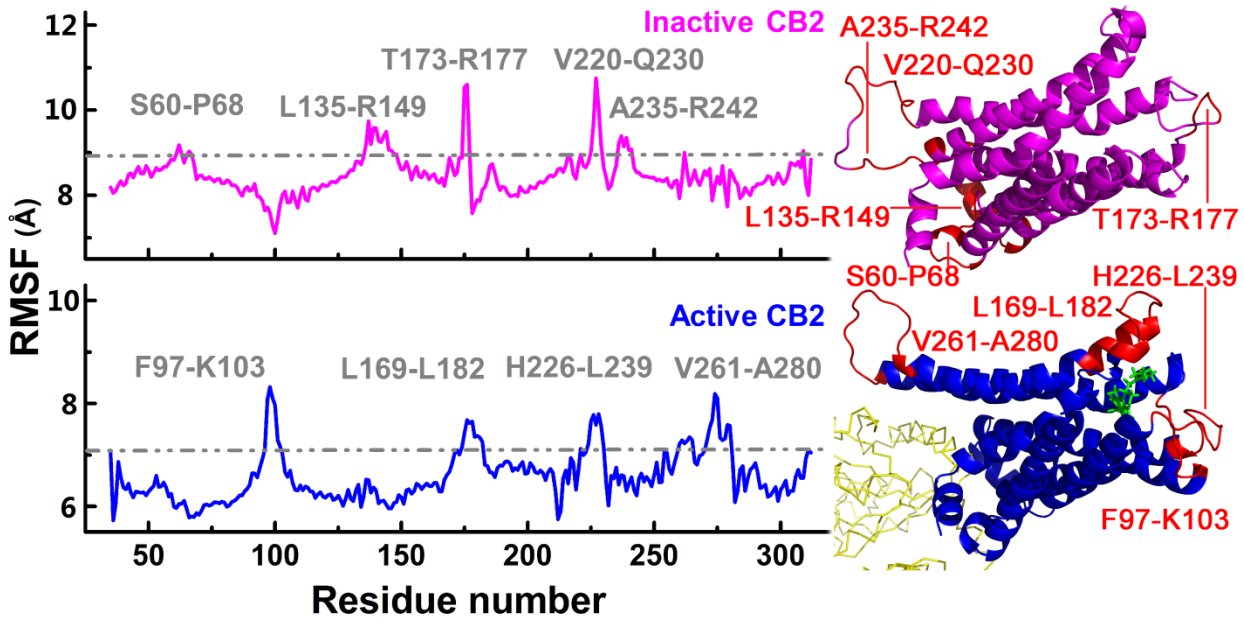

Figure S3. RMSF distributions for both the inactive and active CB2 receptors. (left) RMSF values versus simulation time, (right) 3D structures of the inactive and active CB2 receptors, and the regions with high flexibility were shown in red.

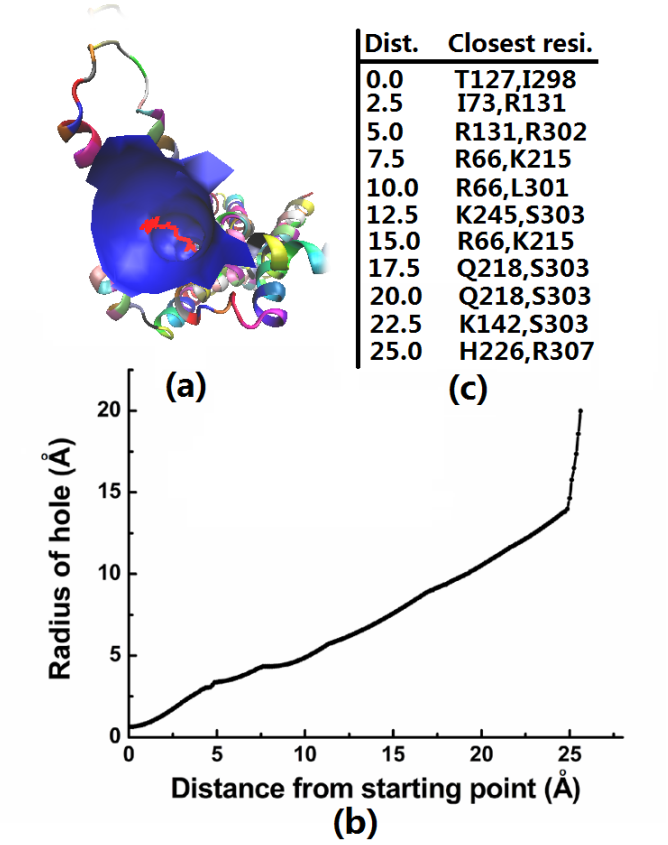

Figure S4. The binding hole of the activated CB2 receptor with G protein. (a) 3D structure of the hole, (b) the radius of hole versus the distance from the initial binding pocket, (c) the closest residues at different distances from starting point.

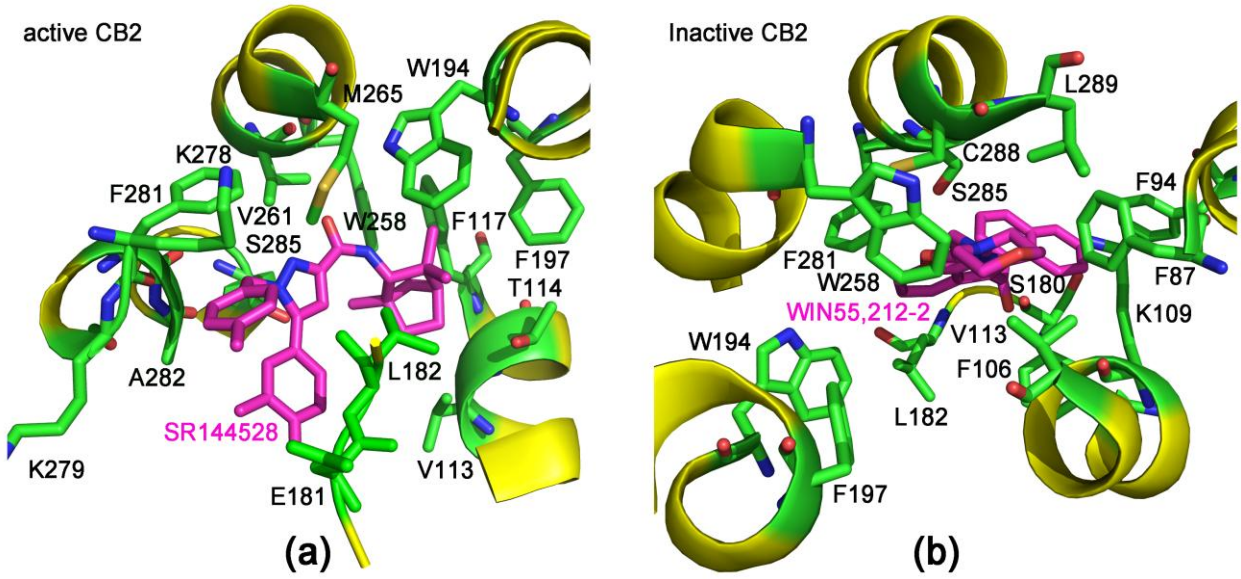

Figure S5. The binding modes of (a) SR144528 with active CB2 and (b) WIN55,212-2 with inactive CB2 model.

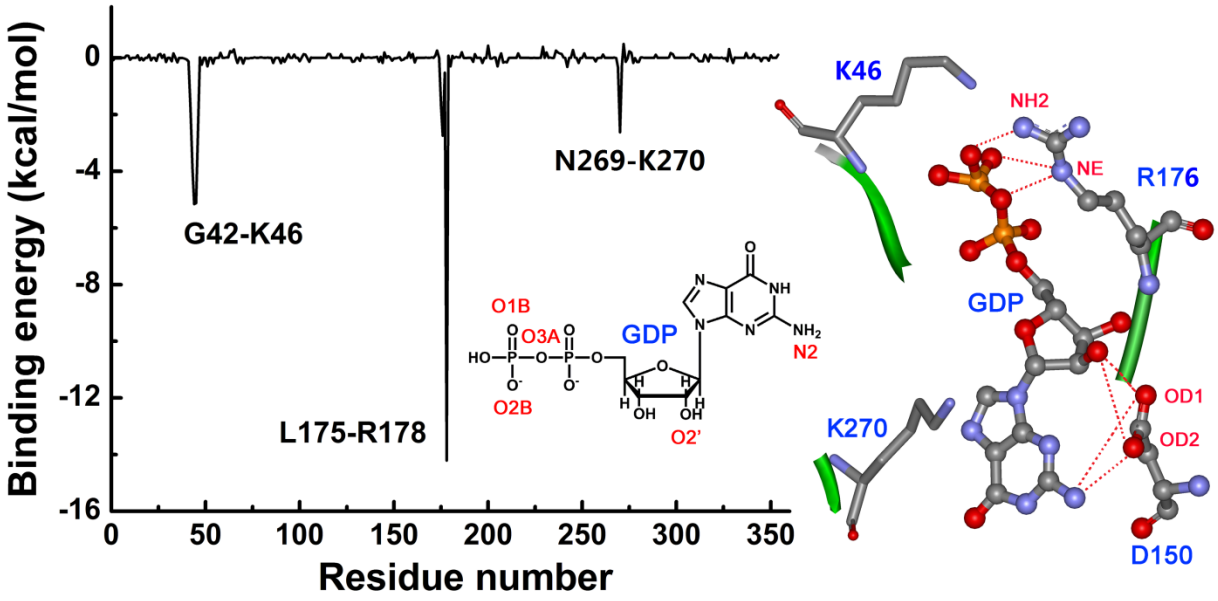

Figure S6. Binding energy contribution of GDP for the association with G_{α} subunit.

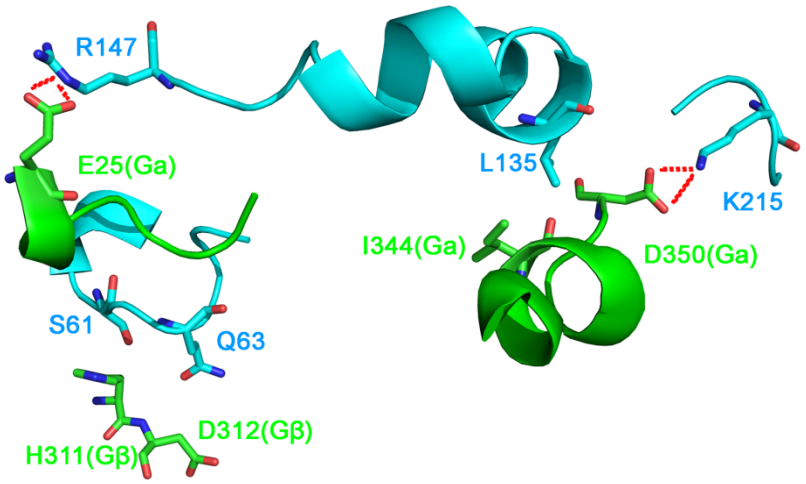

Figure S7. Optimized binding mode between the active CB2 and G proteins after MD simulation.

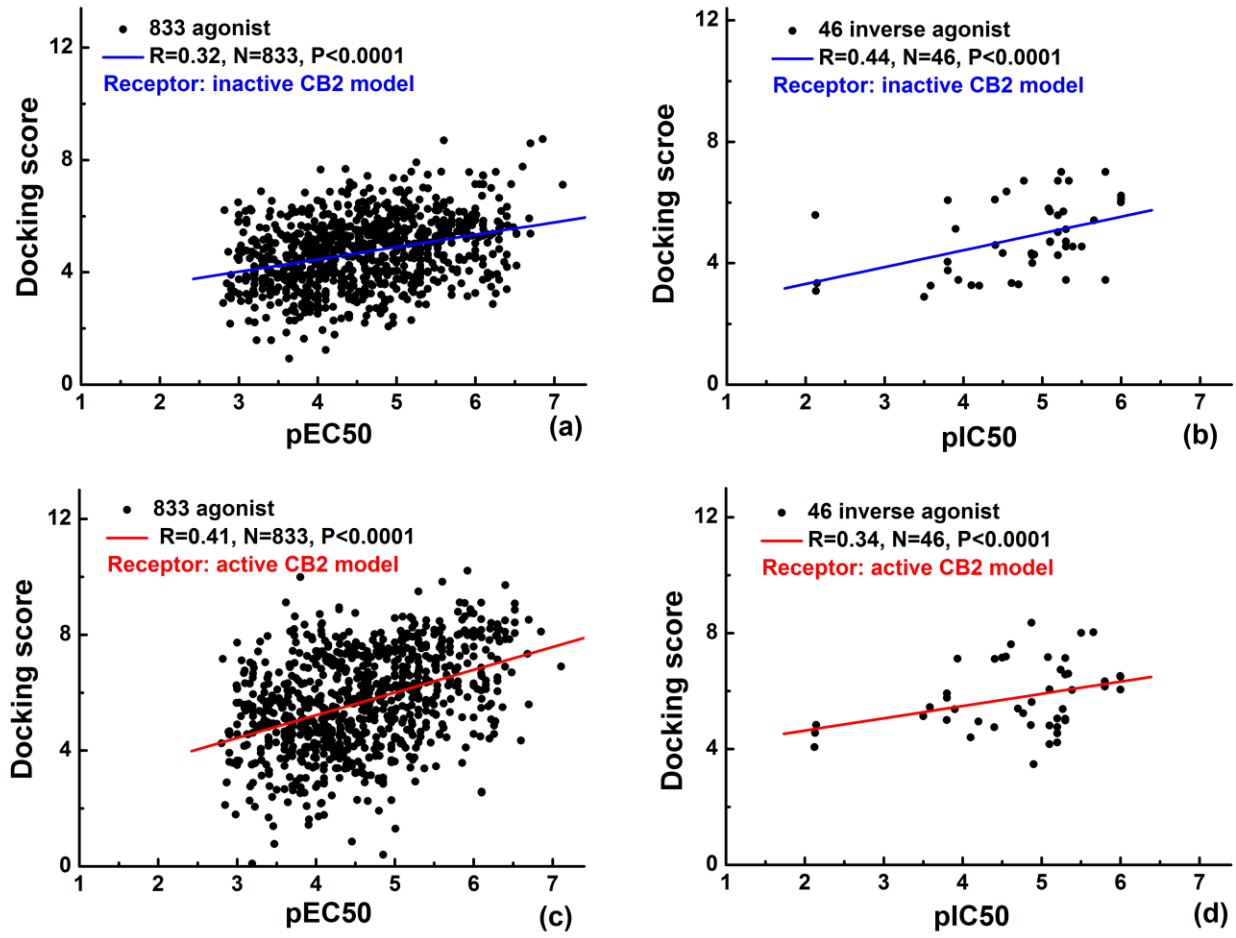

Figure S8. Validation of the active and inactive CB2 models after MD simulations. The first two figures show the correlation between calculated docking scores of inactive CB2 model after MD simulations binding with (a) agonists/ (b) inverse agonists, respectively. (c) and (d) show the same correlations for the active CB2 model .